Signs of conversion in intermediate AMD quantified by deep learning on a population level

Sebastian M. Waldstein, Wolf-Dieter Vogl, Hrvoje Bogunovic, Amir Sadeghipour, Sophie Klimscha, Aaron Osborne, Ursula Schmidt-Erfurth

Department of Ophthalmology, Medical University of Vienna

Purpose: To establish the typical topographic distribution and time course of retinal morphologic changes in intermediate AMD, and to characterize the signs of conversion to advanced AMD.

Methods: We analyzed 10,165 Cirrus SD-OCT scans of 590 patients with intermediate AMD in one eye and neovascular AMD in the fellow eye, who were imaged monthly over two years. To obtain topographic correspondence between patients and over time, all scans were centered at the fovea, rotated such that the optic discs were aligned, and right eyes were mirrored. The time of conversion to CNV and GA was established by two independent, masked retina specialists. Drusen and hyperreflective foci (HRF) were automatically segmented in full 3D using validated deep learning-based methods. Topographically resolved population means of these markers were constructed by averaging drusen and HRF maps in the patient subgroups converting to CNV (n=144), GA (n=75) and in non-converters.

Results: Drusen and HRF showed distinct topographic distribution patterns, with drusen peaking at the foveal center, and HRF peaking at 1°-2° eccentricity with a 2-fold higher prevalence than in the foveal center (Figure 1). Patients converting to advanced disease demonstrated significantly higher drusen and HRF volumes ($p<0.0001$, Table 1). Drusen were more prevalent in CNV converters, and HRF were more prevalent in GA converters. In contrast to eyes converting to CNV, HRF also occurred topographically unrelated to drusen in the GA converters particularly in the parafoveal region ($p=0.039$, Table 1). Eyes progressing to advanced AMD showed a pronounced increase in Drusen and HRF activity prior to conversion.

Conclusion: The classical imaging biomarkers of intermediate AMD, i.e. drusen and HRF, demonstrate distinct topographic patterns. Their distribution and amount also differ markedly between eyes converting to CNV, GA, and non-converters.

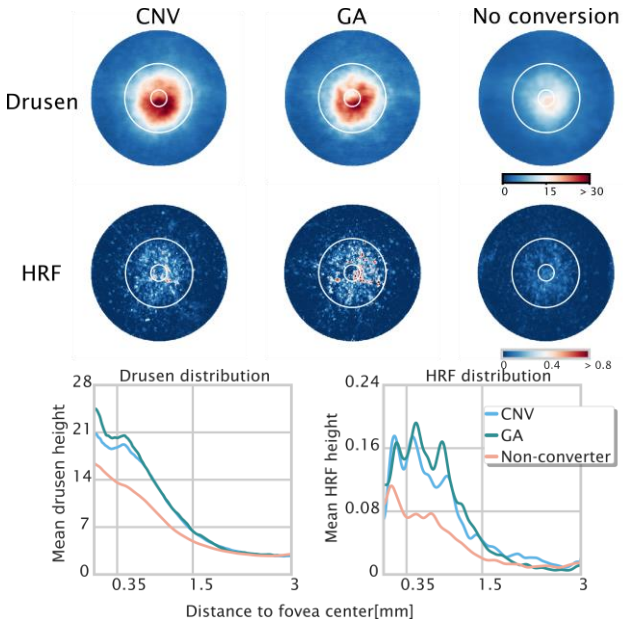

Figure 1: Population-level distributions of drusen and HRF in subgroups developing CNV, GA and non-converters within two years. **(a)** Topographic distribution of drusen and HRF within a 6mm diameter centered on the fovea. **(b)** Frequency distribution of drusen and HRF versus distance to the foveal center.

Table 1: Comparison of drusen and HRF volumes between CNV / GA converters and non-converters (Mann-Whitney rank tests with FDR-Benjamini/Hochberg correction).

Type / Region	CNV vs. non-converter (p-values)	GA vs. non-converter (p-values)	CNV vs GA converter (p-values)
Drusen fovea	**< 0.0001**	**< 0.0001**	0.652
Drusen parafovea	**< 0.0001**	**< 0.0001**	0.465
Drusen perifovea	**< 0.0001**	**< 0.0001**	0.280
HRF fovea	0.082	< 0.0001	0.075
HRF parafovea	**< 0.0001**	**< 0.0001**	**0.001**
HRF perifovea	0.157	0.358	0.905
HRF above drusen fovea	0.044	0.001	0.124
HRF above drusen parafovea	< 0.0001	< 0.0001	**0.012**
HRF above drusen perifovea	0.118	0.118	0.792
HRF not above drusen fovea	0.003	0.775	0.106
HRF not above drusen parafovea	< 0.0001	< 0.0001	**0.039**
HRF not above drusen perifovea	0.628	0.828	0.817